Title	A Model of Driver Steering Control Incorporating Steering Torque Feedback and State Estimation
Authors	Tenghao Niu and David Cole
Number	ENG-TR 005
Date	2020-11-05
ISSN	2633-6839

A Model of Driver Steering Control Incorporating Steering Torque Feedback and State Estimation

Tenghao Niu and David Cole
Department of Engineering, University of Cambridge
E-mail: tn326@cam.ac.uk
21 October 2020

Steering feel, or steering torque feedback plays an important role in the steering control task. In this report, a new driver steering control model incorporating steering torque feedback state estimation is proposed. The hypothesis is that the human driver obtains an internal mental model of the steering and vehicle dynamics, which is used in sensory perception, cognitive control, and neuromuscular action. The new model could be used to predict a driver's responses when steering a vehicle with steering torque feedback.

Keywords: driver-vehicle dynamics, optimal control, state estimation, steering torque feedback

1. INTRODUCTION

Steering feel, or steering torque feedback, is an important aspect of dynamic properties of vehicles and has been devoted significant attention to by vehicle manufacturers. In a real vehicle, lateral forces generated by the tyres on the front axle are communicated to the driver through torque at the steering wheel, and this can give the driver useful information about the vehicle states. Therefore, steering feel not only represents the driver's subjective sensation of steering control, vehicle response and haptic feedback, but also affects the driver's assessment of the vehicle's dynamic qualities upon steering. [1] Although autonomous steering control is a maturing technology, the dynamic interaction between the human occupants and the vehicle is still important and steering torque feedback may play a more significant role in the transition between conventional and automated vehicles. [2]

The report describes a mathematical model of the driver-steering-vehicle system incorporating steering torque feedback and state estimation. Basically, the model comprises the vehicle and steering dynamics, the neuromuscular system, the sensory delays and the human brain functions. The model aims to predict a driver's objective and subjective responses when steering a vehicle with steering torque feedback. The underlying hypothesis is that a human driver obtains an internal mental model of the steering and vehicle dynamics, which is central to the functions of perception, cognition, and action. The model builds on and complements earlier work [3] that focused on modelling the role of vestibular feedback. The derivation of new driver-steering-vehicle model is presented in Section 2, and parameter values for the new model are given in Section 3. Then a sample set of simulation results are presented in Section 4. The main conclusions drawn from the work are summarized in Section 5.

2. DRIVER-STEERING-VEHICLE MODEL

To enable a fundamental understanding of the role of steering torque feedback while reducing the computational cost involved in simulating the model, linear dynamics are used to model the driver-steering-vehicle system in this work. The scope of the model does not extend to speed choice or control, therefore only vehicles travelling at constant longitudinal speed are considered, although the principles behind this model could be extended to include variable-speed vehicles. The driver is assumed to follow a given target path of negligible thickness. A minimal set of human sensory measurements is assumed: visual perception organs and the proprioceptors. The modelling of the vestibular organs is eliminated to reduce the complexity of the study.

The steering task described by the model is represented by Figure 1. Basically, the driver is to follow a randomly moving target path used in [3] in the linear operating regime while compensating for random disturbances acting on the steering and vehicle system. The target path r is straight but randomly varies its lateral displacement from the centreline of the road, which means that the driver does not have any preview of the target path displacement. The aim of this is to ensure that the driver-steering-vehicle system with torque arising from front tyre lateral forces and trail can be disturbed without directly affecting the steering torque feedback. The random disturbances acting on the steering-vehicle system specifically refer to column torque disturbance T_d acting on the steering system, lateral force F_y and yaw moment M_z disturbances acting on the centre of mass of the vehicle. It is assumed that the aim of the driver is to minimise the tracking error between the vehicle lateral displacement and the randomly moving target path.

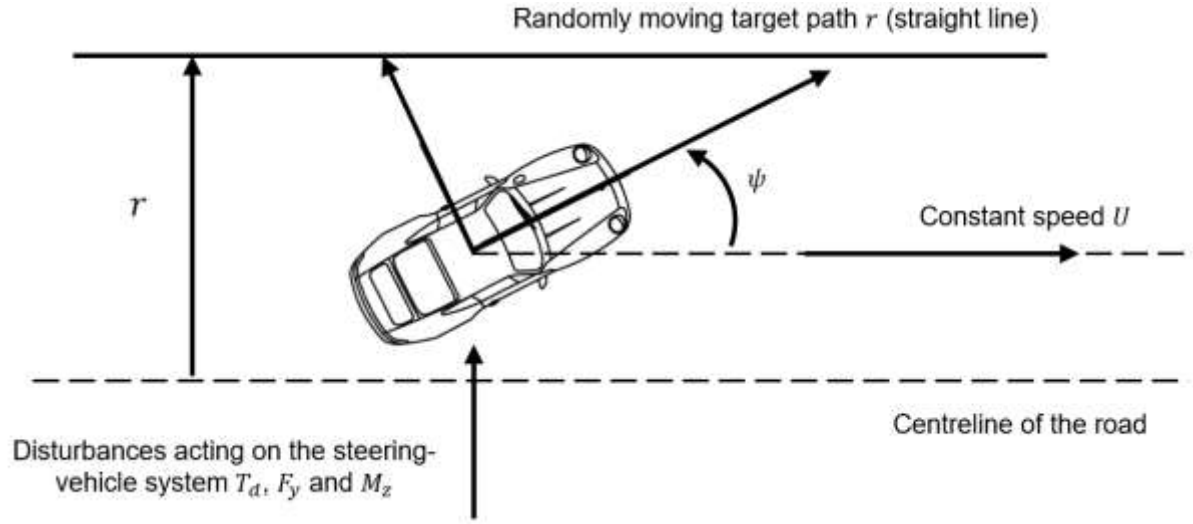

Figure 1: Steering control task described by the new driver model. The driver is to follow the randomly moving target path r while rejecting disturbances acting on the steering-vehicle system T_d, F_y and M_z.

A schematic structure of the new driver-steering-vehicle model is shown in Figure 2. The model is developed based on the hypothesis that the driver is trying to minimise the lateral deviation of the vehicle from the randomly target path by using the optimal estimated states of the plant and the environment from the noisy sensory measurements. The driver's primary control output is the alpha muscle activation signal. The driver's control strategy follows the linear quadratic Gaussian (LQG) framework, combining a linear quadratic regulator (LQR) with a Kalman filter to give statistically optimal control actions and state estimates based on the driver's internal model of the plant. A Kalman filter uses an internal model to achieve optimal state estimation in the presence of additive white noise. However, there is also a muscle stretch reflex action, a stretch reflex (H_r and D_r) controller is therefore also included in this model. The plant shown in Figure 3 describes the plant controlled by the driver in detail, including models of muscle activation process (H_a), the muscle dynamics (part of H_{ms}), the vehicle (H_v) and steering dynamics (the other part of H_{ms}), human sensory delays and disturbance filters (H_{fT}, H_{fF}, H_{fM} and H_{fr}). The perceived states by the driver are the visually-sensed vehicle lateral deviation with respect to the target path e, the yaw angle ψ, and the proprioceptively-sensed muscle angle θ_a.

The driver-steering-vehicle model is implemented as a state-space form, in discrete time with sample period T_s so that delays can be explicitly modelled mathematically. All continuous transfer functions $H(s)$ are converted to discrete state-space matrices (**A**, **B**, **C**, **D**) with states $\boldsymbol{x}$, with subscripts matching the name of that transfer function. Discretisation is carried out using a zero-order hold (ZOH) method. In most cases this is approximated in the form $\mathbf{A} = \mathbf{I} + T_s\mathbf{A}_c$, $\mathbf{B} = T_s\mathbf{B}_c$, where $\mathbf{A}_c$ and $\mathbf{B}_c$ are continuous-time state-space matrices. The time step index is denoted by k.

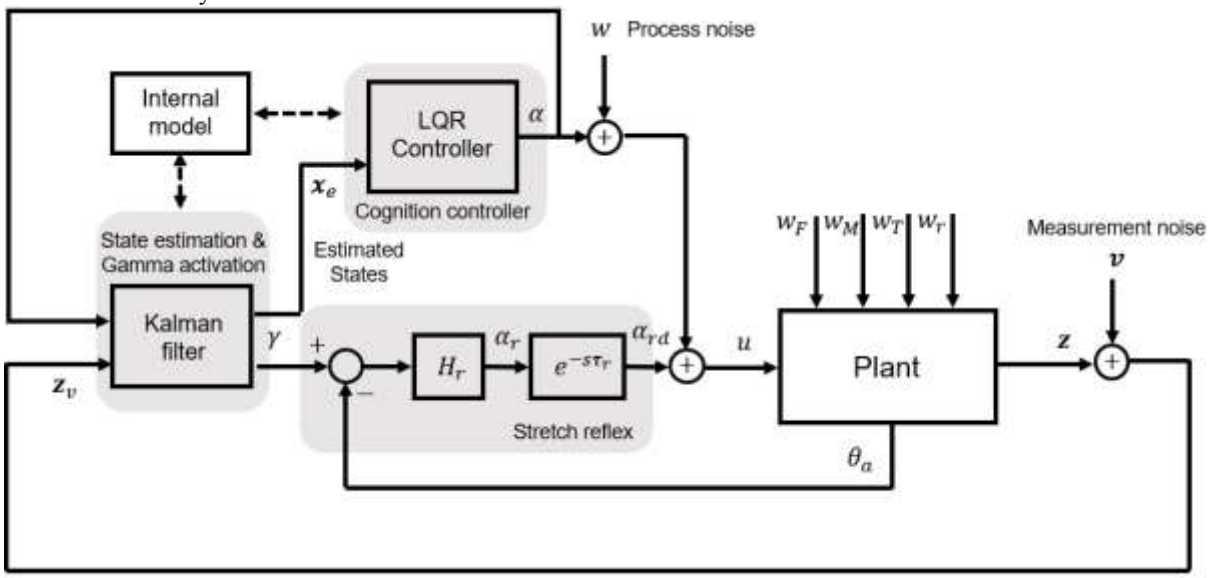

Figure 2: Schematic diagram of the linear driver-steering-vehicle model. Disturbance signals are input as white noise w_F, w_M, w_T and w_r then filtered in the plant. The plant input α and outputs $\boldsymbol{z}$ are perturbed with process

and measurement noise w and $\boldsymbol{v}$, so a Kalman filter estimates the plant states $\boldsymbol{x_e}$. An LQR controller computes an optimal plant input α.

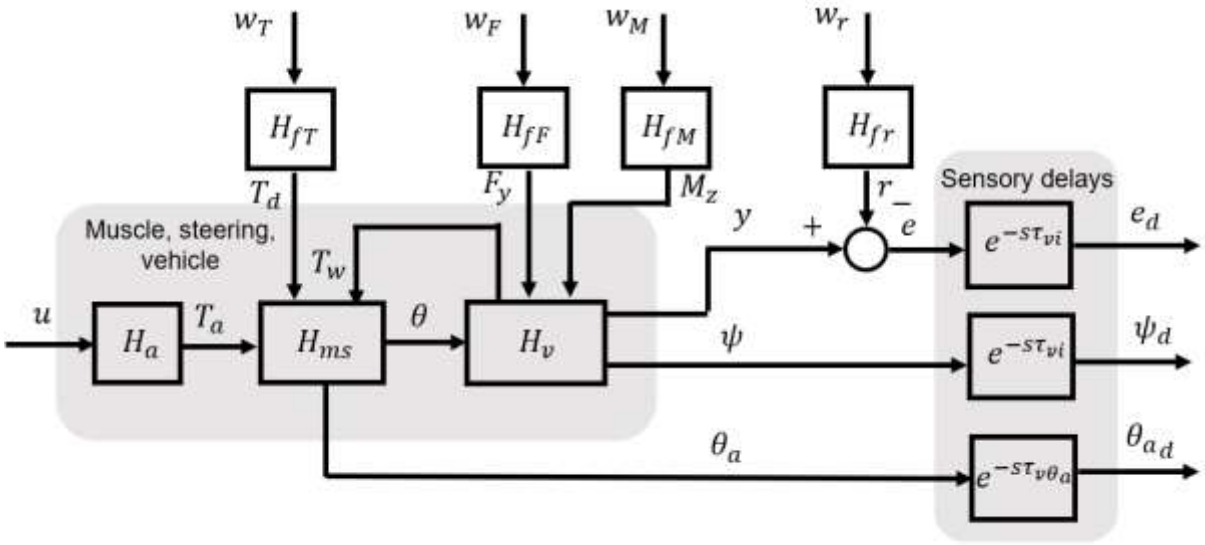

Figure 3: Structure of plant in the new driver-steering-vehicle model. The plant describes the dynamics controlled by the human driver, including muscle activation H_a, muscle and steering dynamics H_{ms}, vehicle dynamics H_v, human sensory delays and disturbance filters H_{fT}, H_{fF}, H_{fM} and H_{fr}.

2.1 VEHICLE MODEL

The vehicle dynamics H_v are represented using the two degree-of-freedom lateral-yaw single-track 'bicycle' model moving at constant speed for simplicity, as shown in Figure 4. The model captures the two dominating motions, i.e. vehicle yaw and lateral motions, with lateral velocity v measured along the lateral axis of the vehicle to the centre of mass of the vehicle and yaw rate ω defined with respect to ground. The yaw angle ψ is defined as the angle between the longitudinal axis of the vehicle and the global x-axis. δ is the front tyres steer angle. The roll and pitch effects of the vehicle are not modelled.

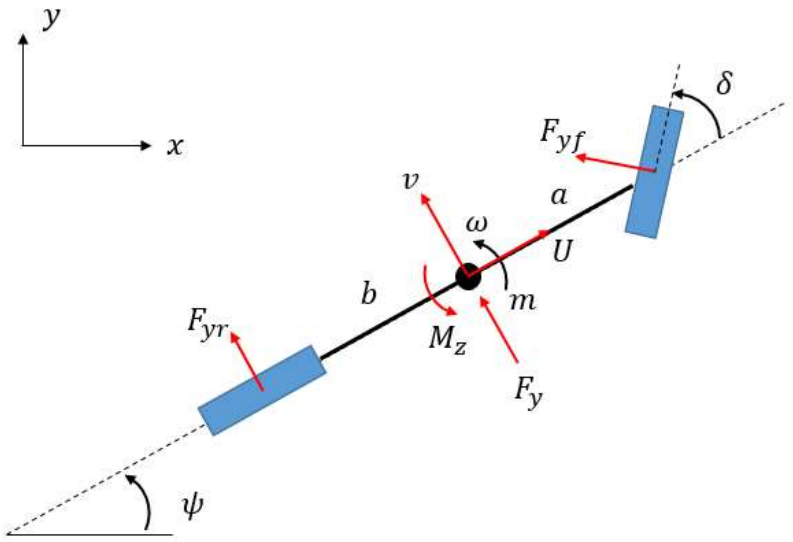

Figure 4: The two degree-of-freedom lateral-yaw vehicle model with disturbance force and moment

For constant longitudinal speed and small-angle assumptions, the equations of motion of the vehicle model are

$$m\big(\dot{v}(t) + U\omega(t)\big) = F_{yf}(t) + F_{yr}(t) + F_y(t) \quad (1)$$

$$I\dot{\omega}(t) = aF_{yf}(t) - bF_{yr}(t) + M_z(t) \quad (2)$$

where U denotes the constant longitudinal speed of the vehicle, m and I denote the vehicle mass and yaw inertia, respectively. a and b denote the distance of front and rear tyres from the centre of mass of the vehicle, respectively.

F_{yf} and F_{yr} are front and rear tyre forces acting along the vehicle lateral axis. A lateral force F_y and a yaw moment M_z applied at the centre of mass of the vehicle act as disturbances, such as might arise from road roughness or wind gusts. For on-centre regime of operation is considered, the lateral tyre forces F_{yf} and F_{yr} are assumed to be proportional to tyre slip angles. Therefore, the lateral forces of the front and rear tyres are

$$F_{yf}(t) = 2C_f\left(\delta(t) - \frac{v(t) + a\omega(t)}{U}\right) \tag{3}$$

$$F_{yr}(t) = 2C_r\left(-\frac{v(t) - b\omega(t)}{U}\right) \tag{4}$$

where C_f and C_r are constant corning stiffness of each front tyre and each rear tyre, respectively. The continuous-time state-space equations of the vehicle model are

$$\begin{Bmatrix}\dot{y}(t)\\ \dot{v}(t)\\ \dot{\psi}(t)\\ \dot{\omega}(t)\end{Bmatrix} = \begin{bmatrix}0 & 1 & U & 0\\ 0 & -\frac{2C_f+2C_r}{mU} & 0 & -U-\frac{2C_fa-2C_rb}{mU}\\ 0 & 0 & 0 & 1\\ 0 & -\frac{2C_fa-2C_rb}{IU} & 0 & -\frac{2a^2C_f+2b^2C_r}{IU}\end{bmatrix}\begin{Bmatrix}y(t)\\ v(t)\\ \psi(t)\\ \omega(t)\end{Bmatrix} + \begin{bmatrix}0 & 0 & 0\\ \frac{2C_f}{m} & \frac{1}{m} & 0\\ 0 & 0 & 0\\ \frac{2C_fa}{I} & 0 & \frac{1}{I}\end{bmatrix}\begin{Bmatrix}\delta(t)\\ F_y(t)\\ M_z(t)\end{Bmatrix} \tag{5}$$

2.2 MUSCLE DYNAMICS AND STEERING MODEL

The muscle dynamics and the steering system are strongly coupled by the torques and angles exchanged through the steering wheel, so they are modelled together as H_{ms}, with the structure shown in Figure 5. The steering dynamics with an assist torque are represented by a two degree-of-freedom system, with the steering wheel angle denoted as θ_{sw} and the steering column angle denoted as θ_c. The linear steering dynamics are interacted with the driver through the introduction of the muscle angle of the arms θ_a resulting from muscle activation driven by neurons. The inertia of the rack and the front wheels referred to the pinion is denoted by I_c. This inertia is connected to the vehicle ground by a torsional stiffness k_{sw} that represents self-centering stiffness (typically arising from the tyre forces acting through the steering geometry) and a parallel torsional damping term c_{sw} that represent the damping in the steering mechanism with respect to the steering wheel axle. The inertia of the steering handwheel is denoted as I_{sw} and the inertia of the driver's arm I_{arm} is assumed to be rigidly connected to the steering wheel, which is denoted by the dashed line between I_{arm} and I_{sw}. The resulting summation of the inertia of the arms I_{arm} and the inertia of the steering wheel I_{sw} are connected with the inertia of the rack and the front wheels I_c by steering column with stiffness k_t and a torsion bar with damping c_t in parallel. Moreover, any additional stiffness and damping effects that may result from steering mechanism referred to the steering wheel are represented by k_{hw} and c_{hw}.

The muscle dynamics considers both the muscle activation and intrinsic dynamics [4]. The mechanical response of the muscle due to change in the steering wheel angle and from neural activation torque is represented by a linearized Hill's muscle model [5], which is a series combination of contractile element (parallel combination of torque from neural activation T_a and a dashpot c_a which resisting stretching of the muscle fibre) and spring k_a representing the elasticity of the tendons. The details of the generation of neural activation T_a are described in later sections. The internal stiffness and damping of the muscles and joints, which are known as muscle intrinsic properties, are fitted by k_p and c_p, respectively.

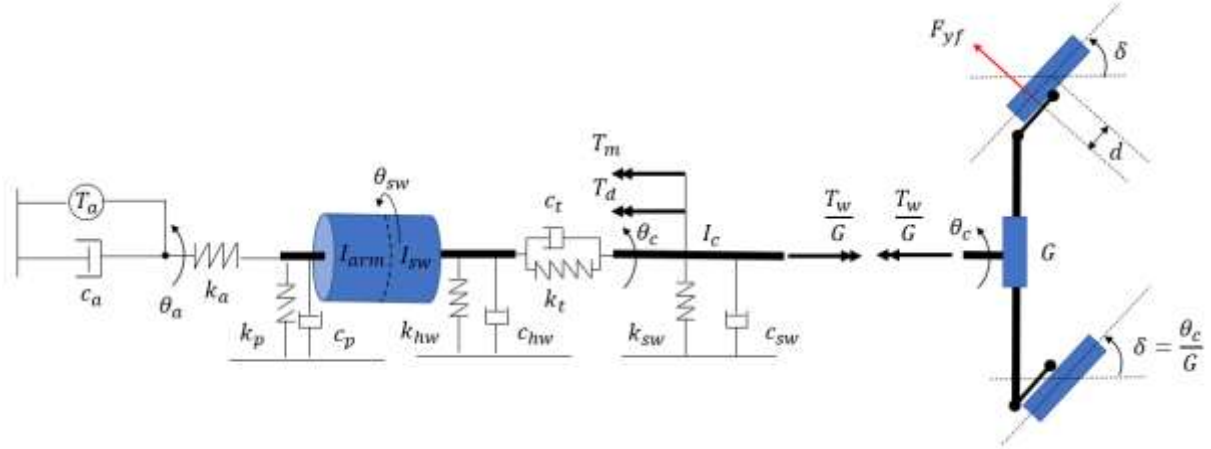

Figure 5: Muscle and steering system model with steering column torque disturbance. The springs and dampers act in rotation.

The equations of motion of the muscle dynamics and steering model are

$$T_a(t) = c_a\dot{\theta}_a(t) + k_a\big(\theta_a(t) - \theta_{sw}(t)\big) \tag{6}$$

$$k_a\big(\theta_a(t) - \theta_{sw}(t)\big) - c_t\left(\dot{\theta}_{sw}(t) - \dot{\theta}_c(t)\right) - k_t\big(\theta_{sw}(t) - \theta_c(t)\big) = (I_{sw} + I_{arm})\ddot{\theta}_{sw}(t) + \big(c_{hw} + c_p\big)\dot{\theta}_{sw}(t) + \big(k_{hw} + k_p\big)\theta_{sw}(t) \tag{7}$$

$$T_d(t) + c_t\big(\dot{\theta}_{sw}(t) - \dot{\theta}_c(t)\big) + k_t(\theta_{sw}(t) - \theta_c(t)) + T_m(t) - \frac{T_w(t)}{G} = I_c\ddot{\theta}_c(t) + c_{sw}\dot{\theta}_c(t) + k_{sw}\theta_c(t) \tag{8}$$

Besides the torque applied by the arm muscles due to muscle activation, the steering model includes the self-aligning moment T_w, the torque input from the driving assist system T_m and the equivalent steering column torque disturbance resulting from the rack. The self-aligning moment T_w due to the torque generated about the king-pin axes by the lateral axle force is given by

$$T_w(t) = F_{yf}(t)d \tag{9}$$

where the front tyre trail distance, consisting both the pneumatic and mechanical trail, is denoted by d. The assist torque applied at the steering column T_m by the driving assist system, assumed to be based on a linear boost curve with boost coefficient C_{boost}, is given by

$$T_m(t) = C_{boost}c_t\big(\dot{\theta}_{sw}(t) - \dot{\theta}_c(t)\big) + C_{boost}k_t(\theta_{sw}(t) - \theta_c(t)) \tag{10}$$

Finally, the steering gear ratio G transforms the steering angle column into the front tyre angle by

$$\delta(t) = \frac{\theta_c(t)}{G} \tag{11}$$

Therefore, the continuous-time state-space equations of the muscle-steering-vehicle is

$$\begin{Bmatrix} \dot{y}(t) \\ \dot{v}(t) \\ \dot{\psi}(t) \\ \dot{\omega}(t) \\ \dot{\theta}_{sw}(t) \\ \ddot{\theta}_{sw}(t) \\ \dot{\theta}_c(t) \\ \ddot{\theta}_c(t) \\ \dot{\theta}_a(t) \end{Bmatrix} = \begin{bmatrix} 0 & 1 & U & 0 & 0 & 0 & 0 & 0 & 0 \\ 0 & -\frac{2C_f + 2C_r}{mU} & 0 & -U - \frac{2C_fa - 2C_rb}{mU} & 0 & 0 & \frac{2C_f}{Gm} & 0 & 0 \\ 0 & 0 & 0 & 1 & 0 & 0 & 0 & 0 & 0 \\ 0 & -\frac{2C_fa - 2C_rb}{IU} & 0 & -\frac{2a^2C_f + 2b^2C_r}{IU} & 0 & 0 & \frac{2C_fa}{GI} & 0 & 0 \\ 0 & 0 & 0 & 0 & 0 & 1 & 0 & 0 & 0 \\ 0 & 0 & 0 & 0 & F_2 & F_3 & F_4 & F_5 & F_1 \\ 0 & 0 & 0 & 0 & 0 & 0 & 0 & 1 & 0 \\ 0 & G_1 & 0 & G_2 & G_3 & G_4 & G_5 & G_6 & 0 \\ 0 & 0 & 0 & 0 & \frac{k_a}{c_a} & 0 & 0 & 0 & -\frac{k_a}{c_a} \end{bmatrix} \begin{Bmatrix} y(t) \\ v(t) \\ \psi(t) \\ \omega(t) \\ \theta_{sw}(t) \\ \dot{\theta}_{sw}(t) \\ \theta_c(t) \\ \dot{\theta}_c(t) \\ \theta_a(t) \end{Bmatrix} + \begin{bmatrix} 0 & 0 & 0 & 0 \\ 0 & \frac{1}{m} & 0 & 0 \\ 0 & 0 & 0 & 0 \\ 0 & 0 & \frac{1}{I} & 0 \\ 0 & 0 & 0 & 0 \\ 0 & 0 & 0 & 0 \\ 0 & 0 & 0 & 0 \\ 0 & 0 & 0 & \frac{1}{I_c} \\ 0 & 0 & 0 & 0 \end{bmatrix} \begin{Bmatrix} T_a(t) \\ F_y(t) \\ M_z(t) \\ T_d(t) \end{Bmatrix} \tag{12}$$

$$\begin{Bmatrix} y(t) \\ \psi(t) \\ \theta_a(t) \end{Bmatrix} = \begin{bmatrix} 1 & 0 & 0 & 0 & 0 & 0 & 0 & 0 & 0 \\ 0 & 0 & 1 & 0 & 0 & 0 & 0 & 0 & 0 \\ 0 & 0 & 0 & 0 & 0 & 0 & 0 & 0 & 1 \end{bmatrix} \begin{Bmatrix} y(t) \\ v(t) \\ \psi(t) \\ \omega(t) \\ \theta(t) \\ \dot{\theta}(t) \\ \theta_c(t) \\ \dot{\theta}_c(t) \\ \theta_a(t) \end{Bmatrix} \tag{13}$$

where $G_1 = \frac{2C_fd}{GUI_c}$, $G_2 = \frac{2C_fad}{GUI_c}$, $G_3 = \frac{(1+C_{boost})k_t}{I_c}$, $G_4 = \frac{(1+C_{boost})c_t}{I_c}$, $G_5 = -\left[\frac{(1+C_{boost})k_t + k_{sw}}{I_c} + \frac{2C_fd}{G^2I_c}\right]$, $G_6 = -\frac{(1+C_{boost})c_t + c_{sw}}{I_c}$, $F_1 = \frac{k_a}{I_{arm}+I_{sw}}$, $F_2 = -\frac{k_a + k_{hw} + k_p + k_t}{I_{arm}+I_{sw}}$, $F_3 = -\frac{c_{hw} + c_p + c_t}{I_{arm}+I_{sw}}$, $F_4 = \frac{k_t}{I_{arm}+I_{sw}}$, $F_5 = \frac{c_t}{I_{arm}+I_{sw}}$

Converted to discrete-time state-space equations with sample period T_s, the above equations become

$$\boldsymbol{x}_{msv}(k+1) = \mathbf{A}_{msv}\boldsymbol{x}_{msv}(k) + \mathbf{B}_{msv}\{T_{a(k)} \quad F_y(k) \quad M_z(k) \quad T_d(k)\}^T \tag{14}$$

$$\{y(k) \quad \psi(k) \quad \theta_a(k)\}^T = \mathbf{C}_{msv}\boldsymbol{x}_{msv}(k) \tag{15}$$

2.3 MUSCLE ACTIVATION

The muscle activation torque T_a arises from the neural activation of the muscle. [4] There are two processes associated with the activation process block H_a shown in Figure 3. Activation begins with a signal u sent to alpha motor neurons in the spine that in turn activate the muscle fibres. The dynamics associated with the motor neurons are represented by a first-order lag with time constant τ_1, which is normally in the range 20-50ms [6]. There is also a lag associated with the activation and deactivation of the muscle fibres. Previous twitch tests found that depending on the muscle size, the activation time constant is 5-15ms while the deactivation time constant is typically in the range 20-60ms. [6] Cole [4] mentioned that it is a necessary approximation for a linear model that a single first-order lag with time constant τ_2 is used for both activation and deactivation of muscle fibres. The series combination of the two first-order lags form the H_a block shown in Figure 3. Therefore, the muscle activation torque T_a relating the signal u is given by the transfer function

$$H_a(s) = \frac{1}{(\tau_1 s + 1)(\tau_2 s + 1)} \tag{16}$$

Converted to state-space form, the muscle activation block H_a is

$$\begin{Bmatrix} \dot{x}_{H_a}(t) \\ \dot{T}_a(t) \end{Bmatrix} = \begin{bmatrix} 0 & -\dfrac{1}{\tau_1\tau_2} \\ 1 & -\dfrac{\tau_1+\tau_2}{\tau_1\tau_2} \end{bmatrix} \begin{Bmatrix} x_{H_a}(t) \\ T_a(t) \end{Bmatrix} + \begin{bmatrix} \dfrac{1}{\tau_1\tau_2} \\ 0 \end{bmatrix} u(t) \tag{17}$$

$$T_a(t) = [0 \quad 1] \begin{Bmatrix} x_{H_a}(t) \\ T_a(t) \end{Bmatrix} \tag{18}$$

Written in matrix notations and converted to discrete-time with sample period T_s, the above state-space equations become

$$\boldsymbol{x}_a(k+1) = \mathbf{A}_a\boldsymbol{x}_a(k) + \mathbf{B}_a u(k) \tag{19}$$

$$T_a(k) = \mathbf{C}_a\boldsymbol{x}_a(k) \tag{20}$$

2.4 SENSORY SYSTEMS

Various sensory systems are used by the driver to infer the states of the vehicle and its surrounding. The main senses used by the driver in the steering control task are visual system, vestibular system and somatosensors. [7] In this work, a minimal set of human sensory measurements is assumed for visual perception organs and the proprioceptors and the modelling of the vestibular organs is considered out of the scope of the research to reduce the complexity of the study. The visual system is not only used for detecting the target path, but also used in perceiving self-motion of the vehicle relative to the surrounding environment. In this work, the perceived states by the visual system are the vehicle lateral deviation with respect the randomly moving target path e and the yaw angle of the vehicle ψ. Proprioceptors are a subset of somatosensors and are used for sense the motion and forces of the joints and muscle, which is an important means the driver has to sense the angle and torque of the steering wheel resulting from the steering dynamics and the contact between the front tyres and the road. In this work, the muscle angle θ_a is included as another measurement. The perceived states are subject to a visual delay τ_{vi} and a muscle sensory delay $\tau_{v\theta_a}$, consisting of $N_{vi} = \tau_{vi}/T_s$ and $N_{v\theta_a} = \tau_{v\theta_a}/T_s$ time steps, respectively. The time delay of cognitive processing is assumed to be lumped together with the sensory delays and not modelled separately. The sensory delays in Figure 3 are implemented using shift registers. The delayed values of the vehicle lateral deviation with respect the randomly moving target path e_d are found by

$$\begin{Bmatrix} e(k) \\ \vdots \\ e(k-N_{vi}+1) \end{Bmatrix} = \begin{bmatrix} \mathbf{0}_{[1,N_{vi}-1]} & 0 \\ \mathbf{I}_{[N_{vi}-1,N_{vi}-1]} & \mathbf{0}_{[N_{vi}-1,1]} \end{bmatrix} \begin{Bmatrix} e(k-1) \\ \vdots \\ e(k-N_{vi}) \end{Bmatrix} + \begin{bmatrix} 1 \\ \mathbf{0}_{[N_{vi}-1,1]} \end{bmatrix} e(k) \tag{21}$$

$$e(k-N_{vi}) = [\mathbf{0}_{[1,N_{vi}-1]} \quad 1] \begin{Bmatrix} e(k-1) \\ \vdots \\ e(k-N_{vi}) \end{Bmatrix} \tag{22}$$

where $\mathbf{I}$ is the identity matrix, $\mathbf{0}$ is a matrix of zeros, and $\mathbf{M}_{[i,j]}$ is a matrix with i rows and j columns. Converted to discrete-time state-space equations with sample period T_s, the above equations become

$$\boldsymbol{x}_{\tau e}(k+1) = \mathbf{A}_{\tau vi}\boldsymbol{x}_{\tau e}(k) + \mathbf{B}_{\tau vi}e(k) = \mathbf{A}_{\tau vi}\boldsymbol{x}_{\tau e}(k) + \mathbf{B}_{\tau vi}\mathbf{C}_{msv(1,:)}\boldsymbol{x}_{msv}(k) - \mathbf{B}_{\tau vi}r(k) \tag{23}$$

$$e(k-N_{vi}) = \mathbf{C}_{\tau vi}\boldsymbol{x}_{\tau e}(k) \tag{24}$$

where $\mathbf{M}_{(i,j)}$ indicates the ith row and jth column of matrix $\mathbf{M}$ and ':' represents the entire row of column of the matrix. Similarly, the delayed values of the vehicle yaw angle ψ_d are found by

$$\boldsymbol{x}_{\tau\psi}(k+1) = \mathbf{A}_{\tau vi}\boldsymbol{x}_{\tau\psi}(k) + \mathbf{B}_{\tau vi}\psi(k) = \mathbf{A}_{\tau vi}\boldsymbol{x}_{\tau\psi}(k) + \mathbf{B}_{\tau vi}\mathbf{C}_{msv(2,:)}\boldsymbol{x}_{msv}(k) \tag{25}$$

$$\psi(k-N_{vi}) = \mathbf{C}_{\tau vi}\boldsymbol{x}_{\tau\psi}(k) \tag{26}$$

The delayed values of muscle angle θ_a are given by

$$\begin{Bmatrix} \theta_a(k) \\ \vdots \\ \theta_a(k-N_{vi}+1) \end{Bmatrix} = \begin{bmatrix} \mathbf{0}_{[1,N_{v\theta_a}-1]} & 0 \\ \mathbf{I}_{[N_{v\theta_a}-1,N_{v\theta_a}-1]} & \mathbf{0}_{[N_{v\theta_a}-1,1]} \end{bmatrix} \begin{Bmatrix} \theta_a(k-1) \\ \vdots \\ \theta_a\left(k-N_{v\theta_a}\right) \end{Bmatrix} + \begin{bmatrix} 1 \\ \mathbf{0}_{[N_{v\theta_a}-1,1]} \end{bmatrix} \theta_a(k) \tag{27}$$

$$\theta_a\left(k-N_{v\theta_a}\right) = \begin{bmatrix} \mathbf{0}_{[1,N_{v\theta_a}-1]} & 1 \end{bmatrix} \begin{Bmatrix} \theta_a(k-1) \\ \vdots \\ \theta_a\left(k-N_{v\theta_a}\right) \end{Bmatrix} \tag{28}$$

Converted to discrete-time state-space equations with sample period T_s, the above equations become

$$\boldsymbol{x}_{\tau\theta_a}(k+1) = \mathbf{A}_{\tau\theta_a}\boldsymbol{x}_{\tau\theta_a}(k) + \mathbf{B}_{\tau\theta_a}\theta_a(k) = \mathbf{A}_{\tau\theta_a}\boldsymbol{x}_{\tau\theta_a}(k) + \mathbf{B}_{\tau\theta_a}\mathbf{C}_{msv(3,:)}\boldsymbol{x}_{msv}(k) \tag{29}$$

$$\theta_a\left(k-N_{v\theta_a}\right) = \mathbf{C}_{\tau\theta_a}\boldsymbol{x}_{\tau\theta_a}(k) \tag{30}$$

The perceived states of the vehicle and its surrounding by the sensory system are then sent to the central nervous system (CNS), subject to measurement noise. These noisy signals are used to estimate the states of plant. The detailed derivation of the state estimator is presented in later sections.

2.5 DISTURBANCE FILTERING

As mentioned earlier in this report, the vehicle moves at constant longitudinal speed U and the driver is asked to follow a randomly moving target path while compensating for disturbances acting on the steering-vehicle system as shown in Figure 3. The target r and disturbances T_d, F_y and M_z are generated by filtering Gaussian white noise to ensure that the closed-loop driver-steering-vehicle system is not excited beyond the frequencies of interest [3]. White noise signals w_r w_F, w_M and w_T are generated in discrete time by choosing random numbers from a zero-mean normal distribution. The corresponding variances W_r^2 W_F^2, W_M^2 and W_T^2 of the signals could be adjusted based on different simulation conditions. Specifically, vehicle lateral force disturbance F_y, vehicle yaw moment disturbance M_z and steering column torque disturbance T_d are generated by passing the noise inputs through second-order low pass filters with cut-off frequency f_{cF}, f_{cM} and f_{cT}, respectively

$$H_{fF}(s) = \left(\frac{f_{cF}}{s+f_{cF}}\right)^2 \tag{31}$$

$$H_{fM}(s) = \left(\frac{f_{cM}}{s+f_{cM}}\right)^2 \tag{32}$$

$$H_{fT}(s) = \left(\frac{f_{cT}}{s+f_{cT}}\right)^2 \tag{33}$$

Converted to state-space form, the above low pass filters are

$$\begin{Bmatrix} \dot{x}_{H_{fF}}(t) \\ \dot{F}_y(t) \end{Bmatrix} = \begin{bmatrix} 0 & -f_{cF}^2 \\ 1 & -2f_{cF} \end{bmatrix} \begin{Bmatrix} x_{H_{fF}}(t) \\ F_y(t) \end{Bmatrix} + \begin{bmatrix} f_{cF}^2 \\ 0 \end{bmatrix} w_F(t) \tag{34}$$

$$F_y(t) = \begin{bmatrix} 0 & 1 \end{bmatrix} \begin{Bmatrix} x_{H_{fF}}(t) \\ F_y(t) \end{Bmatrix} \tag{35}$$

$$\begin{Bmatrix} \dot{x}_{H_{fM}}(t) \\ \dot{M}_z(t) \end{Bmatrix} = \begin{bmatrix} 0 & -f_{cM}^2 \\ 1 & -2f_{cM} \end{bmatrix} \begin{Bmatrix} x_{H_{fM}}(t) \\ M_z(t) \end{Bmatrix} + \begin{bmatrix} f_{cM}^2 \\ 0 \end{bmatrix} w_M(t) \tag{36}$$

$$M_z(t) = \begin{bmatrix} 0 & 1 \end{bmatrix} \begin{Bmatrix} x_{H_{fM}}(t) \\ M_z(t) \end{Bmatrix} \tag{37}$$

$$\begin{Bmatrix} \dot{x}_{H_{fT}}(t) \\ \dot{T}_d(t) \end{Bmatrix} = \begin{bmatrix} 0 & -f_{cT}^2 \\ 1 & -2f_{cT} \end{bmatrix} \begin{Bmatrix} x_{H_{fT}}(t) \\ T_d(t) \end{Bmatrix} + \begin{bmatrix} f_{cT}^2 \\ 0 \end{bmatrix} w_T(t) \tag{38}$$

$$T_d(t) = \begin{bmatrix} 0 & 1 \end{bmatrix} \begin{Bmatrix} x_{H_{fT}}(t) \\ T_d(t) \end{Bmatrix} \tag{39}$$

Written in matrix notations and converted to discrete-time with sample period T_s, the above state-space equations become

$$\boldsymbol{x}_{fF}(k+1) = \mathbf{A}_{fF}\boldsymbol{x}_{fF}(k) + \mathbf{B}_{fF}w_F(k) \tag{40}$$

$$F_y(k) = \mathbf{C}_{fF}\boldsymbol{x}_{fF}(k) \tag{41}$$

$$\boldsymbol{x}_{fM}(k+1) = \mathbf{A}_{fM}\boldsymbol{x}_{fM}(k) + \mathbf{B}_{fM}w_M(k) \tag{42}$$

$$M_z(k) = \mathbf{C}_{fF}\boldsymbol{x}_{fM}(k) \tag{43}$$

$$\boldsymbol{x}_{fT}(k+1) = \mathbf{A}_{fT}\boldsymbol{x}_{fT}(k) + \mathbf{B}_{fT}w_T(k) \tag{44}$$

$$T_d(k) = \mathbf{C}_{fT}\boldsymbol{x}_{fT}(k) \tag{45}$$

The random target path r is generated by passing the noise input w_r through function combing a second-order low pass filter with cut-off frequency f_{rl} and a second-order high pass filter with cut-off frequency f_{rh} [3]

$$H_{fr}(s) = \left(\frac{s}{s+f_{rh}}\right)^2 \left(\frac{f_{rl}}{s+f_{rl}}\right)^2 \quad (46)$$

Similarly, converted to state-space form, and dealt with discrete-time, the transfer function became

$$\boldsymbol{x}_{fr}(k+1) = \mathbf{A}_{fr}\boldsymbol{x}_{fr}(k) + \mathbf{B}_{fr}w_r(k) \quad (47)$$

$$r(k) = \mathbf{C}_{fr}\boldsymbol{x}_{fr}(k) \quad (48)$$

2.6 COMPLETE PLANT

Combing blocks developed from Section 2.1 to 2.5 gives the complete plant, written in discrete-time state-space form

$$\boldsymbol{x}(k+1) = \mathbf{A}\boldsymbol{x}(k) + \mathbf{B}\alpha(k) + [\mathbf{B} \quad \mathbf{G}_r \quad \mathbf{G}_F \quad \mathbf{G}_M \quad \mathbf{G}_T]\{w(k) \quad w_r(k) \quad w_F(k) \quad w_M(k) \quad w_T(k)\}^T \quad (49)$$

$$\boldsymbol{z}(k) = \mathbf{C}\boldsymbol{x}(k) \quad (50)$$

where $\boldsymbol{x}(k) = \{\boldsymbol{x}_{fr}(k) \quad \boldsymbol{x}_{fF}(k) \quad \boldsymbol{x}_{fM}(k) \quad \boldsymbol{x}_{fT}(k) \quad \boldsymbol{x}_{msv}(k) \quad \boldsymbol{x}_a(k) \quad \boldsymbol{x}_{\tau\psi}(k) \quad \boldsymbol{x}_{\tau\theta_a}(k) \quad \boldsymbol{x}_{\tau e}(k)\}^T$,

$\boldsymbol{z}(k) = \{e(k-N_{vi}) \quad \psi(k-N_{vi}) \quad \theta_a(k-N_{v\theta_a})\}^T$,

$$\mathbf{A} = \begin{bmatrix} \mathbf{A}_{fr} & \mathbf{0} & \mathbf{0} & \mathbf{0} & \mathbf{0} & \mathbf{0} & \mathbf{0} & \mathbf{0} & \mathbf{0} \\ \mathbf{0} & \mathbf{A}_{fF} & \mathbf{0} & \mathbf{0} & \mathbf{0} & \mathbf{0} & \mathbf{0} & \mathbf{0} & \mathbf{0} \\ \mathbf{0} & \mathbf{0} & \mathbf{A}_{fM} & \mathbf{0} & \mathbf{0} & \mathbf{0} & \mathbf{0} & \mathbf{0} & \mathbf{0} \\ \mathbf{0} & \mathbf{0} & \mathbf{0} & \mathbf{A}_{fT} & \mathbf{0} & \mathbf{0} & \mathbf{0} & \mathbf{0} & \mathbf{0} \\ \mathbf{0} & \mathbf{B}_{msv(:,2)}\mathbf{C}_{fF} & \mathbf{B}_{msv(:,3)}\mathbf{C}_{fM} & \mathbf{B}_{msv(:,4)}\mathbf{C}_{fT} & \mathbf{A}_{msv} & \mathbf{B}_{msv(:,1)}\mathbf{C}_a & \mathbf{0} & \mathbf{0} & \mathbf{0} \\ \mathbf{0} & \mathbf{0} & \mathbf{0} & \mathbf{0} & \mathbf{0} & \mathbf{A}_a & \mathbf{0} & \mathbf{0} & \mathbf{0} \\ \mathbf{0} & \mathbf{0} & \mathbf{0} & \mathbf{0} & \mathbf{B}_{\tau vi}\mathbf{C}_{msv(2,:)} & \mathbf{0} & \mathbf{A}_{\tau vi} & \mathbf{0} & \mathbf{0} \\ \mathbf{0} & \mathbf{0} & \mathbf{0} & \mathbf{0} & \mathbf{B}_{\tau\theta_a}\mathbf{C}_{msv(3,:)} & \mathbf{0} & \mathbf{0} & \mathbf{A}_{\tau\theta_a} & \mathbf{0} \\ -\mathbf{B}_{\tau vi}\mathbf{C}_{fr} & \mathbf{0} & \mathbf{0} & \mathbf{0} & \mathbf{B}_{\tau vi}\mathbf{C}_{msv(1,:)} & \mathbf{0} & \mathbf{0} & \mathbf{0} & \mathbf{A}_{\tau vi} \end{bmatrix}$$

$\mathbf{B} = [\mathbf{0} \quad \mathbf{0} \quad \mathbf{0} \quad \mathbf{0} \quad \mathbf{0} \quad \boldsymbol{B}_a \quad \mathbf{0} \quad \mathbf{0} \quad \mathbf{0}]^T$

$\mathbf{G}_r = [\mathbf{B}_{fr} \quad \mathbf{0} \quad \mathbf{0} \quad \mathbf{0} \quad \mathbf{0} \quad \mathbf{0} \quad \mathbf{0} \quad \mathbf{0} \quad \mathbf{0}]^T$

$\mathbf{G}_F = [\mathbf{0} \quad \mathbf{B}_{fF} \quad \mathbf{0} \quad \mathbf{0} \quad \mathbf{0} \quad \mathbf{0} \quad \mathbf{0} \quad \mathbf{0} \quad \mathbf{0}]^T$

$\mathbf{G}_M = [\mathbf{0} \quad \mathbf{0} \quad \mathbf{B}_{fM} \quad \mathbf{0} \quad \mathbf{0} \quad \mathbf{0} \quad \mathbf{0} \quad \mathbf{0} \quad \mathbf{0}]^T$

$\mathbf{G}_T = [\mathbf{0} \quad \mathbf{0} \quad \mathbf{0} \quad \mathbf{B}_{fT} \quad \mathbf{0} \quad \mathbf{0} \quad \mathbf{0} \quad \mathbf{0} \quad \mathbf{0}]^T$

$$\mathbf{C} = \begin{bmatrix} \mathbf{0} & \mathbf{0} & \mathbf{0} & \mathbf{0} & \mathbf{0} & \mathbf{0} & \mathbf{0} & \mathbf{0} & \mathbf{C}_{\tau vi} \\ \mathbf{0} & \mathbf{0} & \mathbf{0} & \mathbf{0} & \mathbf{0} & \mathbf{0} & \mathbf{C}_{\tau vi} & \mathbf{0} & \mathbf{0} \\ \mathbf{0} & \mathbf{0} & \mathbf{0} & \mathbf{0} & \mathbf{0} & \mathbf{0} & \mathbf{0} & \mathbf{C}_{\tau\theta_a} & \mathbf{0} \end{bmatrix},$$

$\mathbf{0}$ is a matrix of zeros, $\mathbf{M}_{(i,j)}$ indicates the ith row and jth column of matrix $\mathbf{M}$ and ':' represents the entire row of column of the matrix.

2.7 STRETCH REFLEX CONTROL

The muscle neural activation has been considered to come from the alpha motor neurons in the spine. The alpha motor neurons receive signals from two main sources. [4] Signals can be sent directly from the motor cortex in the brain; in Figure 2 this signal is labelled α. In addition, the alpha motor neurons can be signalled by the reflex action, which is predominantly a closed-loop feedback control of muscle length known as the stretch reflex. Gamma motor neurons in the spine activate special fibres in the muscle called spindles. The motor neurons are believed to adjust the length of the spindles according to the muscle displacement angle (or steering wheel angle) expected by the brain. If the muscle angle differs from the expected angle, the spindles are strained and send a signal to the alpha motor neurons, which in turn activate the muscle to achieve the expected muscle angle. The function of the muscle spindles is represented in Figure 2 by the summation circle, which calculates the difference between the expected angle γ and the actual angle θ_a. The generation of the expected muscle angle γ is presented in later sections. The difference is then operated upon by a reflex gain block H_r and a delay block D_r before activating the muscle via the alpha motor neuron.

In this work, the reflex behaviour is modelled to be sensitive to muscle displacement angle; therefore, the reflex gain block H_r contains a stiffness gain k_r. The reflex delay is largely a function of neural conduction velocities and the distance of the muscle from the motor neurons in the spine. It is modelled as a discrete-time shift register with a parameter τ_r representing the delay time, consisting of $N_r = \tau_r/T_s$ time steps.

$$\begin{Bmatrix} \alpha_r(k) \\ \vdots \\ \alpha_r(k-N_r+1) \end{Bmatrix} = \begin{bmatrix} \mathbf{0}_{[1,N_r-1]} & 0 \\ \mathbf{I}_{[N_r-1,N_r-1]} & \mathbf{0}_{[N_r-1,1]} \end{bmatrix} \begin{Bmatrix} \alpha_r(k-1) \\ \vdots \\ \alpha_r(k-N_r) \end{Bmatrix} + \begin{bmatrix} 1 \\ \mathbf{0}_{[N_r-1,1]} \end{bmatrix} \alpha_r(k) \quad (51)$$

$$\alpha_{rd}(k) = \alpha_r(k-N_r) = [\mathbf{0}_{[1,N_{vi}-1]} \quad 1] \begin{Bmatrix} \alpha_r(k-1) \\ \vdots \\ \alpha_r(k-N_r) \end{Bmatrix} \quad (52)$$

Converted to discrete-time state-space equations with sample period T_s, the above equations become

$$\boldsymbol{x}_{\tau r}(k+1) = \mathbf{A}_{\tau r}\boldsymbol{x}_{\tau r}(k) + \mathbf{B}_{\tau r}k_r[\gamma(k) - \theta_a(k)] \quad (53)$$

$$\alpha_{rd}(k) = \mathbf{C}_{\tau r}\boldsymbol{x}_{\tau r}(k) \quad (54)$$

2.8 KALMAN FILTER FOR STATE ESTIMATION AND GAMMA ACTIVATION

The optimal controller requires the full plant state vector $\boldsymbol{x}$ to calculate the optimal plant input. The sensory systems described in Section 2.4 provide the central nervous system (CNS) with measurements of the plant $\boldsymbol{z}$ of the plant, perturbed by measurement noise $\boldsymbol{v}$, and the CNS could carry out sensory measurement integration using statistically optimal methods to estimate the states of the plant. The process of estimating the states of the plant is represented by using a Kalman filter, based on an internal mental model of the plant derived in Section 2.6, the measurement of noise-free plant input α and noisy measurement $\boldsymbol{z} + \boldsymbol{v}$ of the plant. The theory of Kalman filtering is given by [8] [9]. Initially, an estimate of the states $\boldsymbol{x}_e(k+1|k)$ is predicted by propagating the current input $\alpha(k)$ and state estimate $\boldsymbol{x}_e(k)$ through the internal mental model of the plant

$$\boldsymbol{x}_e(k+1|k) = \mathbf{A}\boldsymbol{x}_e(k) + \mathbf{B}\alpha(k) \quad (55)$$

A correction is then added based on the error between the previous estimated output $\mathbf{C}\boldsymbol{x}_e(k|k-1)$ and measured output $\boldsymbol{z}(k) + \boldsymbol{v}(k)$, weighted by the 'Kalman gain' $\mathbf{K}(k)$

$$\boldsymbol{x}_e(k) = \boldsymbol{x}_e(k|k-1) + \mathbf{K}(k)\{\boldsymbol{z}(k) + \boldsymbol{v}(k) - \mathbf{C}\boldsymbol{x}_e(k|k-1)\} \quad (56)$$

The time-varying Kalman gain $\mathbf{K}(k)$ is calculated to give a statistically optimal minimum-variance estimate based on the concept of 'maximum likelihood estimate' (MLE), weighting the estimates based on the covariances of the Gaussian noise w, w_r, w_F, w_M, w_T and $\boldsymbol{v}$. In this work, the covariances are assumed to be time-invariant, therefore a steady-state Kalman filter is implemented to optimally estimate the states of the plant. The estimate of the plant states $\boldsymbol{x}_e$ is given by

$$\boldsymbol{x}_e(k+1|k) = [\mathbf{A} - \mathbf{LC}]\boldsymbol{x}_e(k|k-1) + [\mathbf{B} \quad \mathbf{L}]\begin{Bmatrix}\alpha(k)\\ \boldsymbol{z}(k) + \boldsymbol{v}(k)\end{Bmatrix} \quad (57)$$

$$\boldsymbol{x}_e(k) = [\mathbf{I} - \mathbf{M}_x\mathbf{C}]\boldsymbol{x}_e(k|k-1) + [\mathbf{0} \quad \mathbf{M}_x]\begin{Bmatrix}\alpha(k)\\ \boldsymbol{z}(k) + \boldsymbol{v}(k)\end{Bmatrix} \quad (58)$$

where gain matrix $\mathbf{L}$ and the innovation gains $\mathbf{M}_x$ and $\mathbf{M}_y$ are

$$\mathbf{L} = \mathbf{APC}^T(\mathbf{CPC}^T + \mathbf{R}_{\mathrm{KF}})^{-1} \quad (59)$$

$$\mathbf{M}_x = \mathbf{PC}^T(\mathbf{CPC}^T + \mathbf{R}_{\mathrm{KF}})^{-1} \quad (60)$$

$$\mathbf{M}_y = \mathbf{CPC}^T(\mathbf{CPC}^T + \mathbf{R}_{\mathrm{KF}})^{-1} \quad (61)$$

and $\mathbf{P}$ is given by solving the following discrete Riccati equation

$$\mathbf{A}^T\mathbf{PA} - \mathbf{P} - \mathbf{A}^T\mathbf{PC}(\mathbf{C}^T\mathbf{PC} + \boldsymbol{R}_{KF})^{-1}\mathbf{C}^T\mathbf{PA} + \widehat{\mathbf{Q}}_{\mathrm{KF}} = \mathbf{0} \quad (62)$$

where $\widehat{\mathbf{Q}}_{\mathrm{KF}} = [\mathbf{B} \quad \mathbf{G}_r \quad \mathbf{G}_F \quad \mathbf{G}_M \quad \mathbf{G}_T]\mathbf{Q}_{\mathrm{KF}}[\mathbf{B} \quad \mathbf{G}_r \quad \mathbf{G}_F \quad \mathbf{G}_M \quad \mathbf{G}_T]$

The process and measurement noise covariance matrices $\mathbf{Q}_{\mathrm{KF}}$ and $\mathbf{R}_{\mathrm{KF}}$ are given by

$$\mathbf{Q}_{\mathrm{KF}} = \mathrm{diag}([W^2 \quad W_r^2 \quad W_F^2 \quad W_M^2 \quad W_T^2]) \quad (63)$$

$$\mathbf{R}_{\mathrm{KF}} = \mathrm{diag}\left(\left[V_e^2 \quad V_\psi^2 \quad V_{\theta_a}^2\right]\right) \quad (64)$$

where W^2 denotes the variance of the process noise w, W_r^2 W_F^2, W_M^2 and W_T^2 denote the variances of the disturbances w_r, w_F, w_M and w_T, respectively, and V_e^2, V_ψ^2 and $V_{\theta_a}^2$ denote the variances of the measurement noise added to the plant outputs e, ψ, and θ_a, respectively.

The generation of the expected muscle angle, labelled as γ in Figure 2, is known as gamma activation, which is also based on an internal mental model of the plant derived in Section 2.6. Specifically, the expected muscle angle γ is calculated by processing the internal mental model of the plant forwardly with the current input $\alpha(k)$ and state estimate $\boldsymbol{x}_e(k)$, which is essentially the prediction step of Kalman filter. Therefore, the gamma activation process is incorporated into the Kalman filter. The expected muscle angle γ is extracted from the initial estimate of the states $\boldsymbol{x}_e(k|k-1)$

$$\gamma(k) = \left[\mathbf{0}_{[1,N_{fr}]} \quad \mathbf{0}_{[1,N_{fF}]} \quad \mathbf{0}_{[1,N_{fM}]} \quad \mathbf{0}_{[1,N_{fT}]} \quad \mathbf{C}_{msv(3,:)} \quad \mathbf{0}_{[1,N_{fa}]} \quad \mathbf{0}_{[1,N_{vi}]} \quad \mathbf{0}_{[1,N_{v\theta_a}]} \quad \mathbf{0}_{[1,N_{vi}]}\right]\boldsymbol{x}_e(k|k-1) \quad (65)$$

where $\mathbf{0}$ is a matrix of zeros, $\mathbf{M}_{[i,j]}$ is a matrix with i rows and j columns, N_i is the number of states in the state vector $\boldsymbol{x}_i(k)$.

2.9 COGNITIVE CONTROLLER

An optimal controller is used to represent the driver's control of steering wheel to follow the randomly moving target path based on the same internal mental model of the plant derived in Section 2.6. The effect of cognitive delay is accounted in the sensory delay blocks and is not considered in this section. A linear quadratic regulator (LQR) and model predictive control (MPC) are the two main implementations of optimal control and have been found to be perform identically when applied under the same circumstance. [10] In this section, an LQR controller is applied for the time-invariant linear plant since it allows the control horizon to be set to infinite. The values of the target and disturbances beyond the prediction horizon are assumed to be Gaussian white noise.

The LQR controller calculates a gain vector $\mathbf{K}_{\mathrm{LQ}}$ which acts on the estimated plant states $\boldsymbol{x}_e$ to give an optimal plant input α, through minimising a cost function J. The additive Gaussian white noise w_r w_F, w_M and w_T are ignored since these are not control actions from the driver. In this work, it is assumed that the driver aligns a different part of the vehicle with the randomly moving target path instead of the centre of vehicle, as illustrated in Figure 6. A time shift constant T_t is included in the model to account for this effect and therefore the cost function J incorporates costs on the shifted lateral deviation of the vehicle from the target path and the plant input α, weighted by q_e and q_α:

$$J = \sum_{k=0}^{\infty} \{q_e[y(k) - r(k) + U\psi(k)T_t]^2 + q_\alpha \alpha(k)^2\} = \sum_{k=0}^{\infty} \{\boldsymbol{x}(k)^T \mathbf{Q}_{\mathrm{LQ}} \boldsymbol{x}(k) + \alpha(k)^T \mathbf{R}_{\mathrm{LQ}} \alpha(k)\} \quad (66)$$

where

$$\mathbf{Q}_{\mathrm{LQ}} = \mathbf{H}^T q_e \mathbf{H} \quad (67)$$

$$\mathbf{H} = \begin{bmatrix} \mathbf{C}_{fr} & \mathbf{0}_{[1,N_{fy}]} & \mathbf{0}_{[1,N_{fz}]} & \mathbf{0}_{[1,N_{fd}]} & 1\ 0\ UT_t & \mathbf{0}_{[1,N_{msv}-3]} & \mathbf{0}_{[1,N_a]} & \mathbf{0}_{[1,N_{vi}]} & \mathbf{0}_{[1,N_{v\theta_a}]} & \mathbf{0}_{[1,N_{vi}]} \end{bmatrix} \quad (68)$$

$$\mathbf{R}_{\mathrm{LQ}} = q_\alpha \quad (69)$$

where $\mathbf{0}$ is a matrix of zeros, $\mathbf{M}_{[i,j]}$ is a matrix with i rows and j columns, N_i is the number of states in the state vector $\boldsymbol{x}_i(k)$. Several previous studies also included the costs on yaw angle error [10] [11], and it is also possible to include the first derivative of the control input with respective time. However only these two elements are involved in the cost function for simplicity in this work. Different combinations of the values of the path-following weightings can represent a range of driving strategies, in particular indicating the trade-off between the path-following accuracy and the control activity to accomplish a driving manoeuvre.

The time-invariant LQR control is of the form [10]

$$\alpha(k) = -\mathbf{K}_{\mathrm{LQ}} \boldsymbol{x}_e(k) \quad (70)$$

where

$$\mathbf{K}_{\mathrm{LQ}} = \left(\mathbf{B}^T \mathbf{S} \mathbf{B} + \mathbf{R}_{\mathrm{LQ}}\right)^{-1} \mathbf{B}^T \mathbf{S} \mathbf{A} \quad (71)$$

and $\mathbf{S}$ is given by solving the following discrete Riccati equation

$$\mathbf{A}^T \mathbf{S} \mathbf{A} - \mathbf{S} - \mathbf{A}^T \mathbf{S} \mathbf{B} \left(\mathbf{B}^T \mathbf{S} \mathbf{B} + \mathbf{R}_{\mathrm{LQ}}\right)^{-1} \mathbf{B}^T \mathbf{S} \mathbf{A} + \mathbf{Q}_{\mathrm{LQ}} = \mathbf{0} \quad (72)$$

Matlab' s 'dlqr' function can be used to evaluate $\mathbf{K}_{\mathrm{LQ}}$ given the costs and the plant being controlled by the human driver.

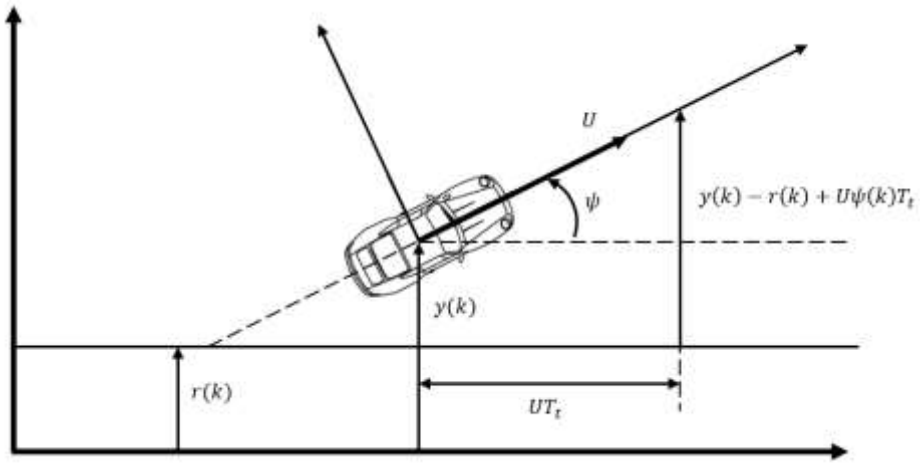

Figure 6: Geometry of driver's viewpoint, a different part of the vehicle is aligned with the randomly moving target path instead of the centre of vehicle.

3. MODEL PARAMETER VALUES

The performance of the new driver-steering-vehicle model depends on the values of the parameters. In total, there are more than forty parameters in the closed-loop driver-steering-vehicle model, including the parameters of the vehicle model, the steering model, and the driver model.

The parameters regarding the steering model and the vehicle model are determined by the dynamic properties of the steering-vehicle system. Most of these parameters are directly given by Toyota Motor Europe (TME) [12] while a small number of them are chosen based on the measured data provide by TME and preliminary stability analysis. The amplitudes of the applied Gaussian white noise and their corresponding filters are determined by the driving conditions.

In general, it is assumed that the driver's internal model matches the actual plant controlled by the driver exactly. Other values relate to physical properties of the human driver; and therefore, work has been carried out

to find suitable values of these driver parameters. Due to the huge number of parameters involved in the driver model, it is necessary to fix the values of some parameters following the results from the relevant literature. To be specific, the muscle activation blocks H_a consists of two time constants in the series of first-order lags τ_1 and τ_2. It has been found that these two time constants are independent of the muscle activation level [6], which means values of them are not affected by the states of the muscle, whether relaxed or tensed. Therefore, it is reasonable to fix the values of them. In this work, a value of 30ms is used for τ_1 and the value of τ_2 is chosen as 20ms, taking the advice of Cole [4]. The reflex delay is also not affected by the muscle activation level and is set to 40ms as suggested by Hoult [6]. However, the intrinsic dynamics of the muscle is affected by the extent to which the muscle is tensed [6]. In this work, the values of intrinsic stiffness k_p and damping c_p are set to 0 $\mathrm{Nm/rad}$ and 0 $\mathrm{Nms/rad}$, respectively for simplicity. The value of tendon stiffness k_a is set to 30 $\mathrm{Nm/rad}$. [5] The visual sensory delay τ_{vi} and the muscle angle sensory delay τ_{θ_a} are set to 0.24s and 0.19s, respectively, guided by the measurement of Nash [13] , who studied drivers' sensory dynamics in steering control task. The values of the LQR controller cost function weightings allow the trade-off between path-following accuracy and control activity to be determined, and it influences the path-following bandwidth of the driver model [6]. This means different driving styles of the driver could be represented by varying the weightings of the cognitive controller cost function. However, it is only the relative weightings that influence the controller performance. Therefore, q_e is set to 1 m^{-2}. The names, symbols, units, and sources of the vehicle model parameters, the steering system parameters and the fixed driver model parameters are summarized in Table 1.

Except the parameters discussed above, there are specifically nine parameters which are neither fixed in advance from relevant literature various nor taken from driving conditions, and therefore, should be identified by using data from experiments. These parameters include the damping c_a resisting stretching of the muscle fibre, the arm inertia I_{arm}, the reflex controller gain k_r, the noise amplitude W, V_e, $V_\psi$and V_{θ_a}, the cognitive controller cost on the shifted lateral deviation of the vehicle from the target path q_e and the controller time shift T_t.

Table 1: Driver-steering-vehicle model parameters

	Description	Parameter	Value	Unit	Source
Vehicle Model	Vehicle mass	m	1370	kg	[12]
	Vehicle yaw moment of inertia	I	1840	kg m^2	[12]
	Lateral front tire stiffness	C_f	41.8×10^3	N/rad	[12]
	Lateral rear tire stiffness	C_r	62.2×10^3	N/rad	[12]
	Distance from CoM to front axle	a	0.98	m	[12]
	Distance from CoM to rear axle	b	1.49	m	[12]
	Longitudinal velocity	U	16.7(60)	m/s(kph)	[12]
Steering Model	Steering gear ratio	G	16		[12]
	Trail (Pneumatic + Caster)	d	0.059	m	[12]
	Stiffness of the steering system due to the kingpin axes (inclination + scrub radius)	k_{sw}	0.516(9)	Nm/rad(Nmm/deg)	[12]
	Moment of inertia of the steering wheel	I_{sw}	0.0264	kg m^2	/
	Damping coefficient of the steering system (of the bearings) and steering system friction	c_{sw}	0.2	Nms/rad	/
	Boost curve coefficient	C_{boost}	0		/
	Steering column stiffness	k_t	115(2)	Nm/rad(Nm/deg)	[1]
	Inertia of the rack and the front wheels referred to the pinion	I_c	$\frac{1.7}{G^2}$	kg m^2	[1]
	Damping coefficient of the torsion bar	c_t	1.74	Nms/rad	/
	Another stiffness term	k_{hw}	0	Nm/rad	/
	Another damping term	c_{hw}	0	Nms/rad	/

Table 1: Driver-steering-vehicle model parameters (continued)

	Description	Parameter	Value	Unit	Source
Driver Model	Intrinsic muscle stiffness	k_p	0	Nm/rad	/
	Intrinsic muscle damping	c_p	0	Nms/rad	/
	Tendon stiffness	k_a	30	Nm/rad	[5]
	Motor neurons lag time constant	τ_1	30	ms	[4]
	Muscle activation and deactivation lag time constant	τ_2	20	ms	[4]
	Visual delay	τ_{vi}	0.24	s	[13]
	Muscle angle sensory delay	τ_{θ_a}	0.19	s	[13]
	Reflex delay	τ_r	40	ms	[6]
	Cost function weight on control input α	q_α	1		/
Simulation setup	Sampling time	t_s	0.02	s	/

4. SIMULATION OF THE DRIVER-STEERING-VEHICLE MODEL

Simulations can be carried out to evaluate the performance of the new driver-steering-vehicle model developed in Section 2. As mentioned earlier, there are nine driver model parameters which are neither fixed in advance from relevant literature nor taken from the driving conditions. A single set of these parameter values is found by conducting identification based on some preliminary experiments over a range of conditions. The details of the identification procedure and the experimental conditions will be reported in another paper. The identified values of these nine parameters are slightly modified to be used in the simulations in this work, as shown in Table 2. Nash and Cole [13] found that the process noise and measurement noise amplitudes in the Kalman filter depend on the RMS values of the equivalent signals in the driver-vehicle-model. However, these signals are not known until after the simulation has been run, so an iterative procedure would be needed to find the RMS signal values for each condition. To save time, these noise amplitudes are simply fixed at the values shown in Table 2 for the simulations. This work is the basis of parameter identification and model validation, which will be carried out in a later work by using the results collected from the driving simulator experiments.

Table 2: Driver model parameters used in the simulations

Description	Parameter	Value	Unit
Damping resisting stretching of the muscle fibre	c_a	3.59	Nms/rad
Arm inertia	I_{arm}	0.056	kgm^2
Reflex gain	k_r	47.2	Nm/rad
Process noise standard deviation	W	6.49	Nm
Standard deviation of measurement noise on lateral deviation of the vehicle from the target path e	V_e	0.1	m
Standard deviation of measurement noise on vehicle yaw angle ψ	V_ψ	0.01	rad
Standard deviation of measurement noise on muscle angle θ_a	V_{θ_a}	0.3	rad
Cognitive controller cost on the shifted lateral deviation of the vehicle from the target path	q_e	2000	
Controller time shift	T_t	0.566	s

In the simulation, instead of being formulated as Gaussian white noises, the disturbances w_r, w_F, w_M and w_T are implemented as step inputs. The simulations are then run with each of these step inputs without process and measurement noises for 10 seconds. The magnitudes of the step inputs and the cut-off frequencies of their corresponding filters are shown in Table 3. The Kalman filter parameters W_r^2, W_F^2, W_M^2 and W_T^2 are set to the equivalent variances of the step inputs used in the simulations. The simulation results of vehicle and driver responses with step input of each of the four disturbances w_r, w_F, w_M and w_T without process and measurement noises are shown in Figure 7 – Figure 10.

Table 3: Magnitudes of the step inputs and cut-off frequencies of the white noise filters used in the simulations

Description	Parameter	Value	Unit
Magnitude of the step input w_r	W_{rs}	1	m
Magnitude of the step input w_F	W_{Fs}	2190	N
Magnitude of the step input w_M	W_{Ms}	2160	Nm
Magnitude of the step input w_T	W_{Ts}	2	Nm
Cut-off frequency for the low-pass filter H_{fF}	f_{cF}	10000	rad/s
Cut-off frequency for the low-pass filter H_{fM}	f_{cM}	10000	rad/s
Cut-off frequency for the low-pass filter H_{fT}	f_{cT}	10000	rad/s
Cut-off frequency for the low-pass filter in H_{fr}	f_{crl}	10000	rad/s
Cut-off frequency for the high-pass filter in H_{fr}	f_{crh}	1×10^{-4}	rad/s

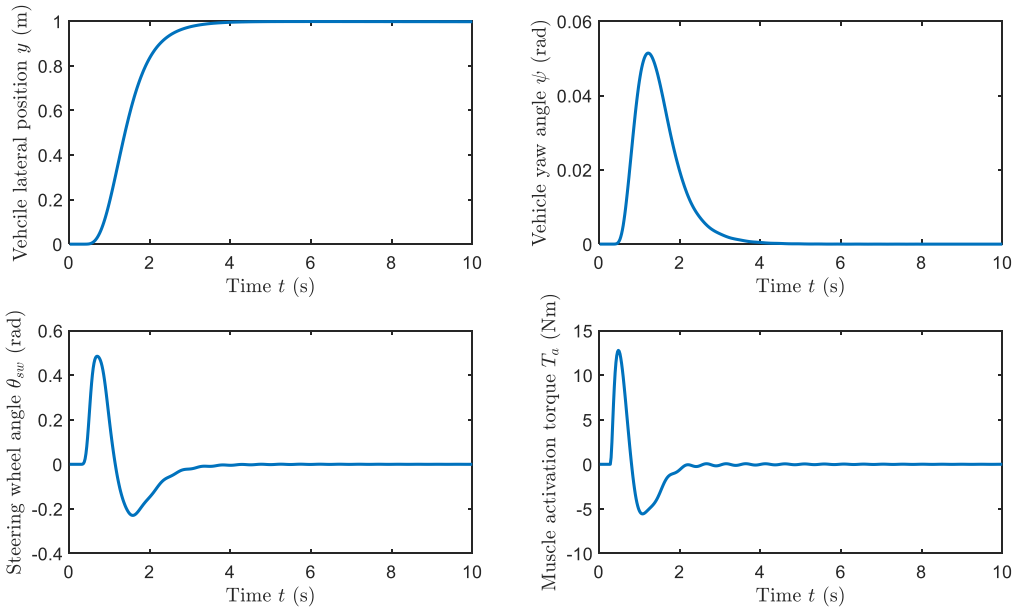

Figure 7: Simulation results of the vehicle and driver responses (vehicle lateral position, vehicle yaw angle, human driver's steering wheel angle and muscle activation torque) with step input of w_r and without process and measurement noises. The step input occurs at t = 0s.

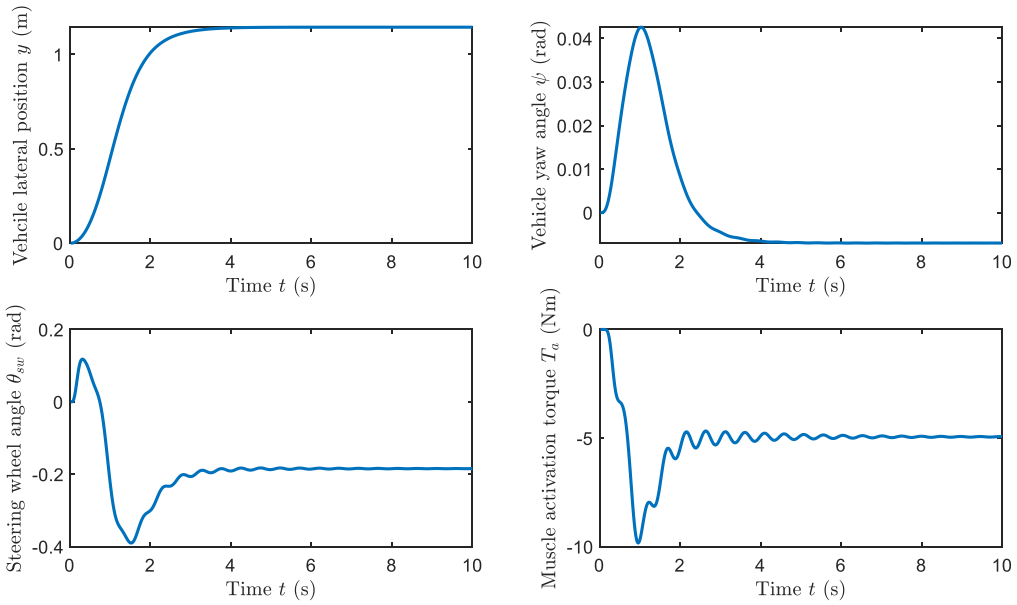

Figure 8: Simulation results of the vehicle and driver responses (vehicle lateral position, vehicle yaw angle, human driver's steering wheel angle and muscle activation torque) with step input of w_F and without process and measurement noises. The step input occurs at t = 0s.

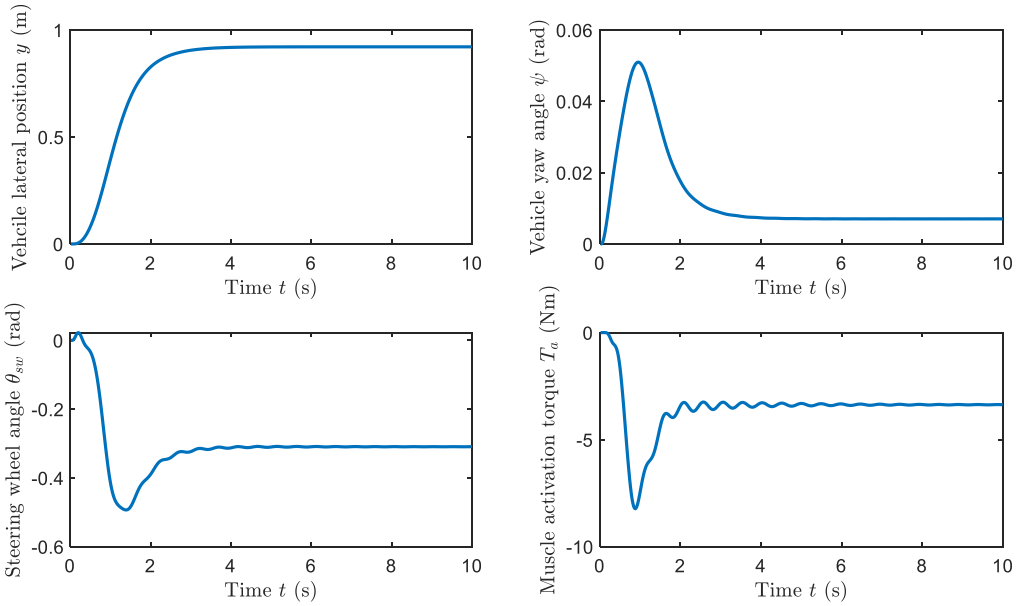

Figure 9: Simulation results of the vehicle and driver responses (vehicle lateral position, vehicle yaw angle, human driver's steering wheel angle and muscle activation torque) with step input of w_M and without process and measurement noises. The step input occurs at t = 0s.

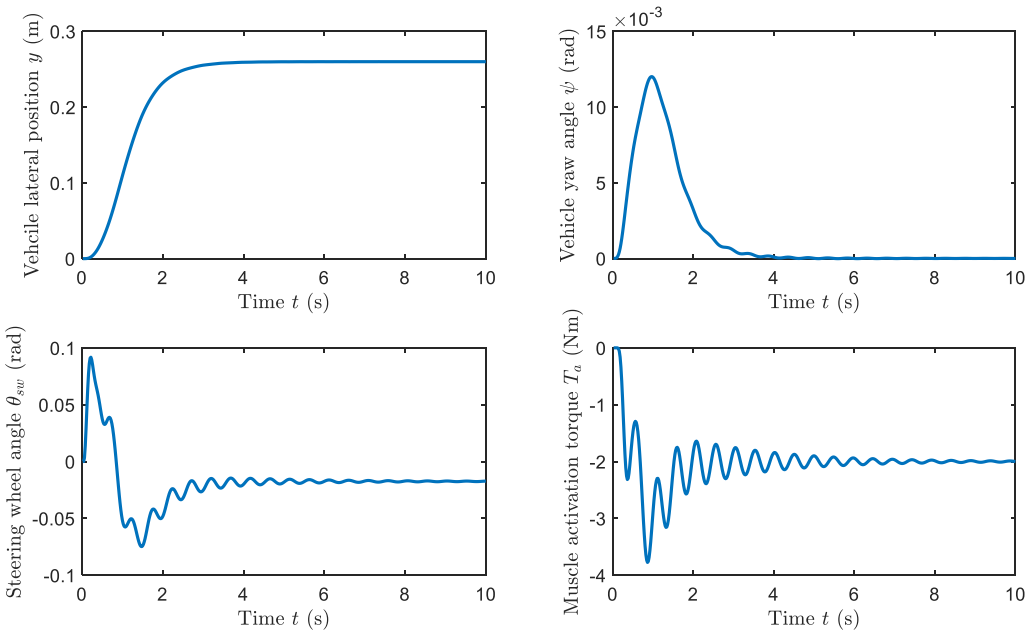

Figure 10: Simulation results of the vehicle and driver responses (vehicle lateral position, vehicle yaw angle, human driver's steering wheel angle and muscle activation torque) with step input of w_T and without process and measurement noises. The step input occurs at t = 0s.

Simulations are then run without any disturbances but with process and measurement noises for 50 seconds. The standard deviation of the process and measurement noises, and cut-off frequency of the white noise filters used in the simulations are shown Table 4. The spectra of the vehicle and driver responses are calculated using a discrete Fourier transform and plotted in Figure 11. The RMS value of the simulated responses are shown in Table 5.

Table 4: Standard deviation of the process and measurement noises and cut-off frequencies of the white noise filters used in the simulations

Description	Parameter	Value	Unit
Standard deviation of the process noise w	W	6.49	Nm
Standard deviation of the measurement noise v_e	V_e	0.1	m
Standard deviation of the measurement noise v_ψ	V_ψ	0.01	rad
Standard deviation of the measurement noise v_{θ_a}	V_{θ_a}	0.3	rad
Cut-off frequency for the low-pass filter H_{fF}	f_{cF}	10000	rad/s
Cut-off frequency for the low-pass filter H_{fM}	f_{cM}	10000	rad/s
Cut-off frequency for the low-pass filter H_{fT}	f_{cT}	10000	rad/s
Cut-off frequency for the low-pass filter in H_{fr}	f_{crl}	10000	rad/s
Cut-off frequency for the high-pass filter in H_{fr}	f_{crh}	1×10^{-4}	rad/s

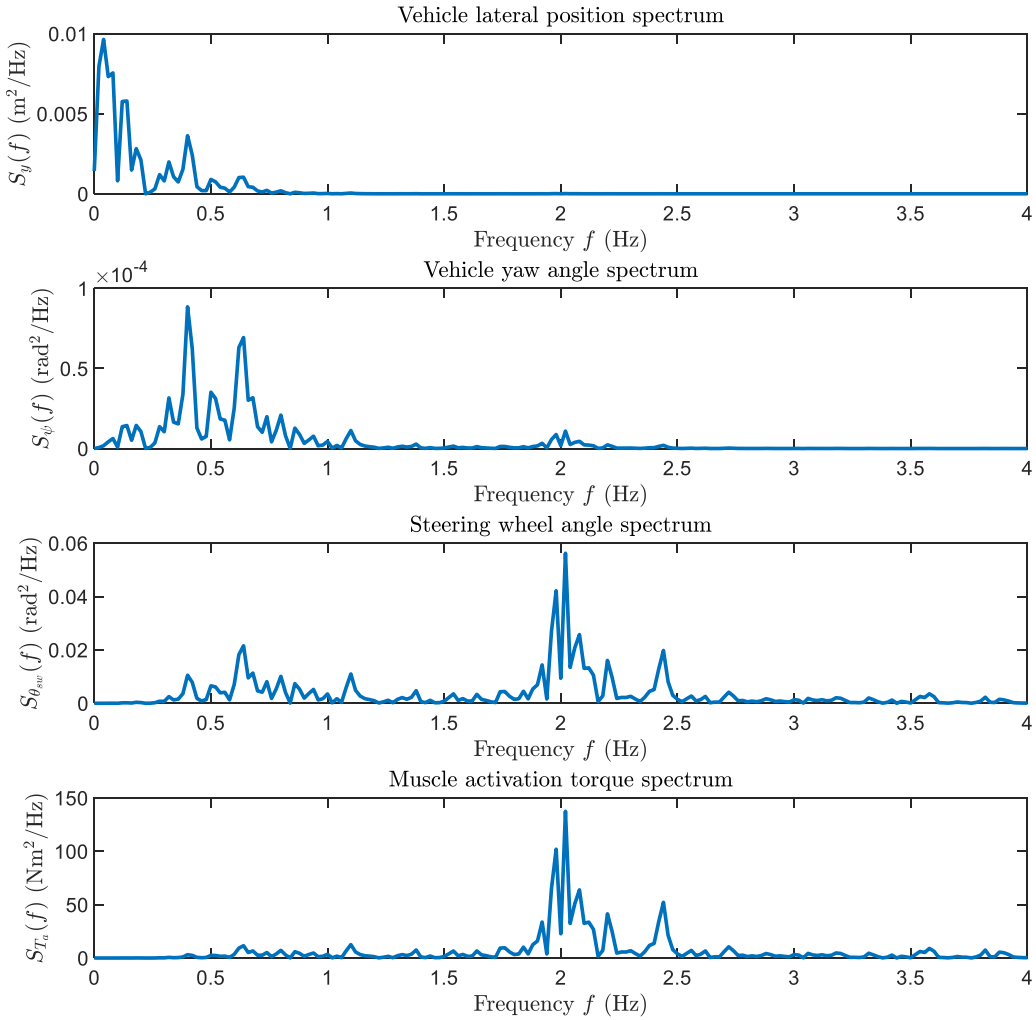

Figure 11: The spectra of the vehicle and driver responses (vehicle lateral position, vehicle yaw angle, human driver's steering wheel angle and muscle activation torque) with process and measurement noises and without any other disturbances.

Table 5: RMS value of the simulated vehicle and driver responses

Description	Value	Unit
RMS value of vehicle lateral position y	0.0350	m
RMS value of vehicle yaw angle ψ	0.0043	rad
RMS value of steering wheel angle θ_{sw}	0.1256	rad
RMS value of muscle activation torque T_a	5.8582	Nm

5. CONCLUSIONS

A linear parametric driver steering control model incorporating steering torque feedback and state estimation has been developed for linear steering dynamics in this report. The novelty of the model is the inclusion of the three important brain functions of perception, cognition and action, all three of which are governed by a single internal model of the plant. In addition, a stretch reflex action is included. The validated model could be used to predict a driver's objective and subjective responses when steering a vehicle with steering torque feedback.

ACKNOWLEDGEMENT

The authors gratefully acknowledge the financial and technical contribution of Toyota Motor Europe (RG88816).

REFERENCES

[1] M. Harrer and P. Pfeffer, Eds., *Steering Handbook*. Cham: Springer International Publishing, 2017.

[2] D. J. Cole, "Occupant–vehicle dynamics and the role of the internal model," *Veh. Syst. Dyn.*, vol. 56, no. 5, pp. 661–688, May 2018.

[3] C. J. Nash and D. J. Cole, "Modelling the influence of sensory dynamics on linear and nonlinear driver steering control," *Veh. Syst. Dyn.*, vol. 56, no. 5, pp. 689–718, May 2018.

[4] D. J. Cole, "A path-following driver–vehicle model with neuromuscular dynamics, including measured and simulated responses to a step in steering angle overlay," *Veh. Syst. Dyn.*, vol. 50, no. 4, pp. 573–596, Apr. 2012.

[5] J. M. Winters and L. Stark, "Muscle models: What is gained and what is lost by varying model complexity," *Biol. Cybern.*, vol. 55, no. 6, pp. 403–420, Mar. 1987.

[6] W. Hoult, "A neuromuscular model for simulating driver steering torque," PhD thesis, University of Cambridge, 2009.

[7] C. J. Nash, D. J. Cole, and R. S. Bigler, "A review of human sensory dynamics for application to models of driver steering and speed control," *Biol. Cybern.*, vol. 110, no. 2–3, pp. 91–116, Jun. 2016.

[8] R. E. Kalman, "A new approach to linear filtering and prediction problems," *J. Fluids Eng. Trans. ASME*, vol. 82, no. 1, pp. 35–45, 1960.

[9] M. S. Grewal and A. P. Andrews, *Kalman Filtering: Theory and Practice Using MATLAB®: Third Edition*. John Wiley and Sons, 2008.

[10] D. J. Cole, A. J. Pick, and A. M. C. Odhams, "Predictive and linear quadratic methods for potential application to modelling driver steering control," *Veh. Syst. Dyn.*, vol. 44, no. 3, pp. 259–284, Mar. 2006.

[11] R. Sharp and V. Valtetsiotis, "Optimal preview car steering control," *Veh. Syst. Dyn.*, vol. 35 (supple, pp. 101–117, 2001.

[12] X. C. Akutain, "Email: Vehicle and steering parameters," *Toyota Motor Europe*, Aug. 2018.

[13] C. J. Nash, "Measurement and Modelling of Human Sensory Feedback in Car Driving," PhD thesis, University of Cambridge, 2018.